HYDROLOGICAL PROCESSES
Hydrol. Process. **28**, 1820–1834 (2014)
Published online 27 February 2013 in Wiley Online Library
(wileyonlinelibrary.com) DOI: 10.1002/hyp.9709

Nitrate dynamics in a rural headwater catchment: measurements and modelling

Philip J. Smethurst,[1]* Kevin C. Petrone,[2] Günter Langergraber,[3] Craig C. Baillie,[1] Dale Worledge[1] and David Nash[4]

[1] *CSIRO Ecosystem Sciences, CRC for Forestry, and Landscape Logic CERF, Private Bag 12, Hobart TAS 7001, Australia*
[2] *CSIRO Land and Water, and Landscape Logic CERF, Private Bag 5, Wembley WA 6913, Australia*
[3] *Institute of Sanitary Engineering and Water Pollution Control, University of Natural Resources and Life Sciences (BOKU), Muthgasse 18, A-1190 Vienna, Austria*
[4] *Department of Primary Industries, 1301, Hazeldean Road, Ellinbank VIC 3821, Australia*

Abstract:

This study was designed to improve our understanding of, and mechanistically simulate, nitrate (NO_3) dynamics in a steep 9.8 ha rural headwater catchment, including its production in soil and delivery to a stream via surface and subsurface processes. A two-dimensional modelling approach was evaluated for (1) integrating these processes at a hillslope scale annually and within storms, (2) estimating denitrification, and (3) running virtual experiments to generate insights and hypotheses about using trees in streamside management zones (SMZs) to mitigate NO_3 delivery to streams. Total flow was mathematically separated into quick- and slow-flow components; the latter was routed through the HYDRUS software with a nitrogen module designed for constructed wetlands. Flow was monitored for two years. High surface-soil NO_3 concentrations started to be delivered to the stream via preferential subsurface flow within two days of the storm commencing. Groundwater NO_3-N concentrations decreased from 1.0 to less than 0.1 mg l^{-1} from up-slope to down-slope water tables, respectively, which was attributed to denitrification. Measurements were consistent with the flushing of NO_3 mainly laterally from surface soil during and following each storm. The model accurately accounted for NO_3 turnover, leading to the hypotheses that denitrification was a minor flux (<3 kg N ha^{-1}) compared to uptake ($98^{-}127$ kg N ha^{-1}), and that SMZ trees would reduce denitrification if they lowered the water table. This research provides an example of the measurement and modelling of NO_3 dynamics at a small-catchment scale with high spatial and temporal resolution. Copyright © 2013 John Wiley & Sons, Ltd.

KEY WORDS forest; hydrology; nitrogen cycling; pasture; stream flow; water quality

Received 30 August 2012; Accepted 7 January 2013

INTRODUCTION

Nitrate (NO_3) concentrations in stream water and annual rates of export are of concern for down-stream uses including potable water, livestock production, aquaculture, irrigation, and the provision of natural habitat in rivers and estuaries. Agricultural production in many regions of the world occurs in conjunction with high rates of atmospheric or fertilizer nitrogen (N) inputs. This leads to NO_3 concentrations in stream and ground waters exceeding recommended or allowable levels. Hence, during the past few decades, there has been interest in understanding landscape processes that deliver NO_3 to streams (Rasiah *et al*., 2010; Rozemeijer *et al*., 2009; Shabaga and Hill, 2010; Zhu *et al*., 2011).

When attempting to understand, simulate, and predict temporal patterns of concentrations and annual export rates of NO_3 from a catchment, it is important to conceptualize spatially and temporally both the sources and transport mechanisms that result in NO_3 delivery to the stream. This conceptualization phase has been reported already for many catchments and has shown, for instance, that the concentration–discharge patterns of NO_3 depend predominantly on the contributions of overland-, inter-, and baseflow to water flow and NO_3 concentrations. Because rainwater commonly has a low concentration of NO_3, major overland flow events can be expected to dilute higher-NO_3-concentration water that seeps from the subsoil and dominates base-flow conditions (Rusjan *et al*., 2008; Holz, 2010). However, if rainwater percolates through the soil and interflow dominates, high-concentration water can be mobilized and rapidly delivered to the stream during and shortly after a storm. This process has been referred to as NO_3 flushing (Creed and Band, 1998). Over longer time periods (weeks to months), high-NO_3 surface water also percolates slowly down the soil profile in predominantly a vertical direction and recharges groundwater, which in-turn leads to seasonal changes in the concentration of NO_3 in baseflow (Rusjan *et al*., 2008). Flushing leads to a positive relationship between flow and NO_3 concentration seasonally (Ohrui and Mitchell, 1998; Ohte *et al*., 2001; Chiwa *et al*., 2010) or within rainfall events (Poor and McDonnell, 2007). Within-event patterns can change from a concentration pattern to a dilution pattern due to season (Petrone *et al*., 2007), contaminant

*Correspondence to: Philip J. Smethurst, CSIRO Ecosystem Sciences, CRC for Forestry, and Landscape Logic CERF, Private Bag 12, Hobart TAS 7001, Australia.
E-mail: Philip.Smethurst@csiro.au

(Holz, 2010), or land use (Poor and McDonnell, 2007). NO_3 concentrations in baseflow may be high or low compared to storm flow, depending on the relative sources and mobilization of NO_3 in soil *versus* ground water.

Patterns of concentration–discharge can be simulated using three-end-member mixing models if concentrations in the end members are known and their relative contributions to flow can be deduced from tracers or by other means (Evans and Davies, 1998; Katsuyama *et al*., 2001; Petrone *et al*., 2007). However, such models do not account for landscape processes that lead to the flow or concentration inputs required for the model. A need to quantitatively model landscape processes that produce and deliver NO_3 to streams has already led to more mechanistic models, e.g. Hill-vi (Weiler and McDonnell, 2006), JAMS/J2000-S (Kralisch and Krause, 2006; Krause *et al*., 2006), SINIC (Hong *et al*., 2006), and SWIM (Huang *et al*., 2009). Yet, these approaches focus mainly on large catchment outcomes, and none have attempted to simulate within-soil water and solute behaviour using the Richard's equation for saturated–unsaturated water flow, and Fickian-based advection–dispersion equations for solute transport. The combination of these mechanisms currently provides the most mechanistic approach available for simulating water and solute transport in soil profiles (Šimůnek *et al*., 2008).

The HYDRUS software incorporates these mechanistic water flow and solute transport equations and can be used in one-, two-, or three-dimensional applications with preferential flow and other options (Šimůnek *et al*., 2008). Its 2D application includes a model describing N dynamics (i.e. the CW2D biokinetic model of the HYDRUS wetland module) developed for simulating NO_3 removal from effluent in constructed wetlands (Langergraber and Šimůnek, 2005, 2012), but this module had not been evaluated for use on soils, hillslopes, or small catchments that were not completely flooded. Although the HYDRUS wetland module was of interest for this application, it was not designed to simulate the down-slope temporal dynamics and solute composition of overland flow. This limitation could potentially be overcome by identifying a quick (overland)-flow and slow-flow component of total flow using an acceptable mathematical procedure of flow analysis (e.g. Lyne and Hollick, 1979), and routing the slow-flow component through the HYDRUS software to later be discharged to the stream as the combination of base- and inter-flow components.

In Australia and internationally, few studies have sought to understand and simulate NO_3 and water dynamics at the headwater catchment scale, yet it is in headwater catchments that most NO_3 is generally delivered to streams and where water quality is poorest (Weaver *et al*., 2001). The use of streamside management zones (SMZs, also called vegetated buffer strips and riparian buffers; Neary *et al*., 2010) that contain trees and shrubs is widely accepted as an option for mitigating nonpoint source pollution on farms (Tilman *et al*., 2002; Dosskey *et al*., 2010; Zhang *et al*., 2010). Some authors have speculated that adding trees to SMZs will add carbon to the system and promote denitrification (Rassam *et al*., 2008). However, trees might also increase transpiration rates in this zone, and thereby lower water tables and reduce denitrification. Under such conditions, N uptake by trees might be of greater importance than denitrification for enhancing NO_3 mitigation. To better integrate our understanding of NO_3 uptake by plants and microbes with catchment scale hydrological processes, we need mechanistic models that operate in at least two dimensions (hillslope transect), and with enough flexibility to conduct virtual experiments in various types of catchments and climatic scenarios (Stutter *et al*., 2012). We saw the HYDRUS wetland module as possibly providing such a capability and therefore explored its use.

The objectives were to combine field measurements and modelling of N cycling processes to: 1) quantify the major pools and fluxes of water and NO_3 in a small rural headwater catchment, 2) evaluate a method of modelling these processes during storm events and annually using flow analysis in combination with the CW2D biokinetic model of the HYDRUS wetland module (i.e. HYDRUS-CW2D), and, if this evaluation was favourable, 3) use this model to estimate ecosystem denitrification, simulate virtual experiments, and thereby develop a working hypothesis on the potential effects of SMZs containing deep-rooted trees.

MATERIALS AND METHODS

Site

The study area was a north-facing headwater catchment (9.8 ha) of Forsters Rivulet, which flows into the Huon River in southern Tasmania, Australia. Land use is grazing (68%) in the lower part, and native forest (32%) in the upper part (Figure 1). Farmer records indicate average annual rainfall (1991–2006) was 722 mm (range 501–975 mm; ca. 5th percentile mm rainfall 551, 10th 560, 50th 709, 90th 913, 95th 990). The catchment is in steep terrain (average 17^{o} slope). Soils are 2–3 m deep, derived from interlaid and mixed slope deposits of Cretaceous syenite and Permian mudstone. The 0–0.2 m soil horizon is a dark brown silty loam and moderately well structured. Clay and grit contents increase with depth to a gritty medium or heavy clay texture at 2–3 m depth. Syenite rock fragments are present in profiles throughout the catchment, and the presence of mudstone fragments increases from none at the top of the catchment (exposed syenite rock) to being the dominant rock fragment on the western boundary of the catchment. Surface-soil (0–10 cm depth; < 2 mm) properties were loam or clay-loam textures with 0.7–1.0 g cm^{-3} bulk density, 0.081 dS m^{-1} electrical conductivity (1:5 soil:water), 5.5 pH_{water}, 0.46 mg kg^{-1} total N, 16 carbon (C):N, 40.8 mg kg^{-1} available-phosphorus (P) (Colwell), 17.5 meq 100 g^{-1} effective cation exchange capacity, and 94% base saturation (Rayment and Higginson, 1992). The soil fraction < 2 mm was 51–99% in surface-soil samples, but only 1% in some samples at the bottom of the profile (3 m).

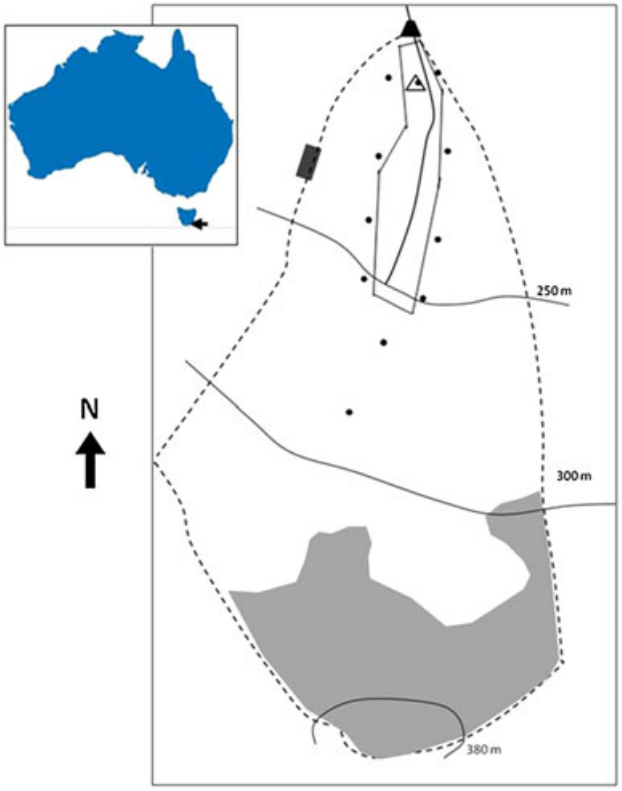

Figure 1. Map of Australia showing the location of the study site (indicated by arrow in the inset map), and map of the study site showing the locations of catchment boundary (broken line), stream (bold solid line), contours (solid lines with elevations indicated), vegetation types (shaded is forest, blank is pasture, irregular block around the stream marked by a solid line is the fenced SMZ plantation), weather station (shaded rectangle), weir (solid trapezoid), TDR instrument (triangle), and piezometers (circles)

For the year preceding the study (2007), the catchment was irregularly grazed within a general regime of moderate stocking density (c. 2–3 head per ha) for 2–6 week periods at 2–3 month intervals. Cattle had free access to all unfenced streams. A mixed-species plantation was established in 2008 in the 5–30 m variable-width fenced SMZ. The area of the SMZ (0.6 ha) was 6% of the catchment and 10% of the pasture area in the catchment. Within the SMZ, soil outside the saturated riparian zone was cultivated by a 'scoop-and-pile' method using a mini-excavator, which created a pit adjacent to a mound on which a tree seedling was planted. Tree seedlings were planted in August 2008. In the lower, northern half of the SMZ, *Eucalyptus nitens* (shining gum) was planted on each mound, and *Acacia melanoxylon* (blackwood) was planted in the saturated riparian zone. In the top, southern half of the SMZ, *Eucalyptus globulus* (blue gum) was planted on each mound top, and there was no saturated riparian zone. Fertilizers were not used in the catchment for several years prior to or during the study, except during plantation establishment in the SMZ. The pasture consisted of grasses and non-leguminous dicotyledons. Within 2 months of planting, all eucalypt seedlings received weed control and 200 g of diammonium phosphate (17.5% N 20.0% P; equivalent of 5.1 kg N and 5.8 kg P ha^{-1} for the total catchment), which was split between two spade slits in the soil about 15 cm on opposite sides of the planting position. The overall stocking of the plantation was 1419 trees ha^{-1}.

Measurements

An automatic weather station was installed on the boundary of the catchment in 2007 that recorded rainfall. Annual rainfall at the site was 603 mm for 2007, 501 mm for 2008, and 879 mm for 2009. On two occasions, rainwater was sampled over a period of 3 days into a clean plastic funnel and bottle, and analysed for NO_3 as described below for other water samples.

A 60^{O}, aluminium plate, V-notch weir was installed at the outlet of the catchment in early 2008 and included water level readings with a capacitance probe recording every 5 min. Water level was converted to flow using a standard rating curve equation for 60° V-notch weirs. NO_3 and other parameters were monitored every three to six weeks using one grab sample taken from each weir. An automatic sampler was used to sample stream water every few hours for several days during three storms (Table I). Samples were analysed for NO_3 using the colorimetric cadmium reduction method on a flow-injection analyser (Lachat Method 12-107-04-1-F).

Volumetric soil water content in the SMZ was measured hourly by time domain reflectometry at several locations in a 200 m^2 area of the SMZ. Probes ($n = 3$) were placed at 0–15 cm, 30–45 cm, and 60–75 cm. Due to equipment failure, these measurements were made for several 3-week periods during the 2008 and 2009, rather

Table I. Summary of rainfall and stream flow during the three storms that were automatically sampled during 2009

	Storm 1	Storm 2	Storm 3
Rainfall			
Start date	13th May	3rd June	26th November
Duration (d)	5	4	5
Total (mm)	33.4	38.4	30.4
Peak Intensity (mm 15 min^{-1})	1.2	1.4	2.2
Flow			
Average (kl d^{-1})	18.6	117.6	28.5
Peak (kl d^{-1})	35.5	241.4	68.6
Day of peak	3	3	3
Peak:initial	17.6	37.8	279.1

than the entire period. Soil in this location was representative of the SMZ.

NO_3 in soil water was sampled using two methods. Soil water held at low tension (leachate) was sampled using inert porous suction samplers (Prenart©). Nine were installed in three zones across the hillslope, i.e. upper mid-slope pasture, lower mid-slope pasture, and in the SMZ (buffer), for *in situ* sampling of leachate. Samplers were placed 45° from vertical and at 75 cm depth (i.e. below the root zone of pasture). Water samples were collected over periods of 1–3 d and refrigerated in the laboratory at 4 °C for up to 14 d prior to NO_3 analysis. Leachate samples could be collected only when the soil was quite wet, and not all samplers yielded soil water at each attempt. At similar locations to the leachate samplers, piezometers were installed to measure water table depths and NO_3 concentrations (method as for stream water samples). Water removal prior to sampling was found to be unnecessary. Dissolved oxygen was measured at various depths in the water table at four locations on one date (April 2009) using a galvanic probe.

Soil water was also sampled using a paste method (Smethurst *et al*., 1997), from which concentrations of NO_3 in soil solution were estimated (analysis as for stream water samples). Surface-soil samples (0–10 cm depth) were collected on three occasions (September 2009 to March 2010) from three zones across the catchment (up-slope forest, mid-slope pasture, and low-slope pasture-plantation SMZ). At each sample location, 20 soil cores were bulked per sample analysed.

Annual rates of net N mineralization and nitrification for the 0–10 cm depth were estimated using aerobic incubations and the SNAP model that was developed for temperature Australian conditions (Paul *et al*., 2002). The measurements were based on three incubated cores per location and 15 sampling locations covering the same zones as those used for soil solution sampling. Cores were sampled when relatively moist (September 2009) and incubated at 27.5° C for 30 d. Nitrification in the 0–10 cm depth was assumed to be half of that occurring for the total soil profile (Moroni *et al*., 2004).

Pasture vegetation was sampled periodically from 0.25 m^2 quadrates ($n = 3$) within animal-excluded area near the weir and the weather station. Samples were oven-dried (70° C), weighed, ground, and analysed for total N (Lowther, 1980).

Modelling

The HYDRUS software (Šimůnek *et al*., 2008; version 1.05) was used in a two-dimensional, sloped, rectangular (trapezoidal) configuration. The model can be accessed at: http://www.pc-progress.com/en/Default.aspx?hydrus-3d. Units used were cm for length, d for time, and mg l^{-1} for concentration. An atmospheric (precipitation) boundary condition was specified for the surface, with a vertical seepage face at the bottom of the slope, and no-transfer boundaries for other faces. Seepage refers to water movement out of a soil profile at a face with an atmospheric boundary condition (saturation excess) and can include components of interflow soon after rainfall, stored soil water, and ground water entering the soil profile from an aquifer. Runoff was defined as overland flow in excess of infiltration, seepage as the combination of baseflow and interflow, and stream flow as seepage plus runoff. No seepage into basement rock was assumed.

In order to simulate hillslope processes in two dimensions, an average hillslope length was calculated as catchment area divided by twice the stream length. A total of 1197 spatial nodes were used (96 lateral by 21 vertical). The spacing of lateral and vertical nodes was closest at the lower slope and surface-soil zones. Time steps started at very low values (0.0001 d) and increased during stable periods to a maximum of 1 d. Evaporation was included in the potential evapotranspiration flux based on that estimated by the weather station. Before rainfall events were simulated, a pre-simulation included runs (up to 200 d) of average rainfall and solute inputs that enabled an effective steady state to be achieved for seepage rate and concentration. Simulated seepage and runoff fluxes were in two-dimensional units (cm^2 d^{-1}) and converted to three-dimensional output by multiplying by the length of the third dimension (catchment length = catchment area/length of hillslope = 2 × measured stream length).

Previously, two methods of simulating runoff were tested, i.e. rainfall that is instantaneously in excess of infiltration (method A), and the use in HYDRUS of a hypothetical layer at the top of the soil profile with extremely high porosity and hydraulic conductivity (method B). However, neither of these overland flow methods was able to adequately simulate the short-term temporal dynamics of stream flow during rainfall events (Smethurst *et al*., 2009). Instead, a third method was developed in the current study whereby measured stream flow was analysed mathematically by the Lyne and Hollick (1979) method (i.e. flow analysis) to estimate the quick-flow and slow-flow components, which approximate to overland flow and inter- plus baseflow, respectively. As the slow-flow component had to originate from rainfall, it was routed through HYDRUS as precipitation. Resultant seepage estimated by HYDRUS was combined with the quick-flow component in a post-HYDRUS spreadsheet to estimate stream flow. Also, in the spreadsheet, NO_3 in seepage (as simulated by HYDRUS) and NO_3 in runoff (as user-prescribed values) were combined to provide an estimate of NO_3 in stream flow. In this manner, flow and solute dynamics in the May storm event (storm 1; Table I) were simulated using inputs summarized in Table II.

For an annual period of NO_3 transformations (i.e. nitrification and denitrification), the CW2D biokinetic model was used with HYDRUS, along with measured daily rainfall and potential evapotranspiration. The CW2D model was designed primarily to simulate NO_3 removal from effluent waters draining through variably flooded constructed wetlands (Langergraber and Šimůnek,

Table II. Description of the simulated May storm: salient HYDRUS inputs

Attribute	Value
General Description	Hillslope as for catchment 1 in photo 1, with tuned water balance. Deep roots (native forest) for top 38% of slope. Shallow roots (pasture) for lower 62% of slope.
Slope length (m)	515.2
Duration (d)	7
Water fluxes	Hourly rainfall and potential transpiration assuming no evaporation
Root water uptake	Feddes model parameters (no solute stress): P0 -10, POpt -25, P2H -300, P2L -1000, P3 -1100, r2H 0.5, r2L 0.1
Spatial nodes	Horizontal: 96 (2.5 m apart at the bottom of slope to 5.7 m apart at the top of slope) Vertical: 21 (0.027 m apart at the top of the soil profile to 0.27 m apart at the bottom of the soil profile)
Time steps (d)	10^{-7}–10^{-3}
HYDRUS units	cm length, mg l^{-1} liquid concentration, mg kg^{-1} solid concentration, g cm^{-3} soil bulk density
Slope (^{O})	17.4
Rainfall (mm)	33.4
Soil horizons: thickness (m), texture[1], K_{sat} (cm d^{-1})	Horizon 1: 0.24, sandy loam, 3×10^{5}; Horizon 2: 0.23, sandy loam, 106.1; Horizon 3: 2.55, silty clay, 0.48
Root depths (m)	3.0:0.5:0.5 for native forest: pasture: SMZ
Initial NO_3-N concentrations	Surface soil (0–0.5 m depth) had 0.082 mg l^{-1} at 0–0.1 m depth and 0.0082 mg l^{-1} at 0.1–0.4 m depth, except for a the bottom 0.5–10.0 m of the hillslope, which contained a NO_3 hot spot (7 mg l^{-1} at surface decreasing linearly to 0.0082 mg l^{-1} at 0.4 m depth). Subsoil (0.5 to 3.0 m depth) contained 0.082 mg l^{-1} NO_3.

2005) by accounting for changes in microbial biomass, organic matter, and some inorganic pools of N and P. The dynamics of 13 solutes (oxygen, three fractions of organic matter, four microbe species, ammonium (NH_4), nitrite (NO_2), NO_3, dinitrogen (N_2), phosphate (PO_4), and an inert tracer) are simulated using nine processes. For this application of HYDRUS, complexity was reduced by artificially fixing the depth-dependent concentrations of O_2 and NH_4 using high values of their respective solid–liquid phase partition coefficients. The option of including temperature dependency of reactions was not used, and simulations were conducted using a measured average annual soil temperature (12.5 °C). Inputs for simulating this catchment are summarized as scenario 1 in Tables III and IV. HYDRUS-CW2D outputs were post-processed in a spreadsheet to estimate annual fluxes and pool changes for water and NO_3. Specification of the grazing or plantation management regime in the SMZ was limited to root depth and therefore evapotranspiration. While management regime can affect water use, such details were beyond the scope of this study.

Scenario 1 and four additional scenarios were used to simulate potential SMZ plantation effects (Tables III and IV):

- Scenario 1: SMZ pasture (not plantation) with roots to 0.5 m depth. Native forest in the top half of the catchment was assumed to have roots of the same water uptake properties, but extending to 3.0 m depth.
- Scenario 2: an SMZ plantation replaced the pasture within 25 m of the stream. The plantation was simulated by extending root depth from 0.5 m to 3.0 m.
- Scenario 3: an SMZ plantation was not included, but conditions were more conducive to denitrification than scenario 1.
- Scenario 4: an SMZ plantation was added to scenario 3.
- Scenario 5: as for scenario 4, but with double the width of plantation, more carbon input and soil drying from it.

RESULTS

Rainfall and stream flow

The flow season was defined as starting at the beginning of May each year, as this approximated the end of the dry period with low flows. During the two-year period May 2008 to April 2010, 572 mm of rain fell during the first flow season and 814 mm during the second. It rained every month, with a minimum of 16.6 mm in May 2008 and maximum of 133.4 mm in September 2009. June–October 2009 was the wettest four-month period, but otherwise there was no apparent trend in monthly rainfall (data not presented). Hence, the first year of the study was relatively dry and the second relative wet, which resulted in relatively low and higher stream flow, respectively (Figure 2). Daily rainfall peaked at 39.4 mm on 27th September 2009, and maximum daily rainfall during sampled storms was 11.8–17.4 mm. Two storms were sampled May–June 2009, which were the first major storms after the dry period, and which marked the start of the second flow season. A third storm was sampled in November 2009, i.e. near the end of major flow of the second season. Of the storms sampled, total storm rainfall ranged from 30.4 to 38.4 mm (Table I).

Table III. Description of annual scenarios: salient HYDRUS inputs

Attribute	Scenario 1	Scenario 2	Scenario 3	Scenario 4	Scenario 5
General Description	Hillslope as for study catchment (Figure 1), with tuned water balance, nitrification and NO_3 uptake. Model estimates of denitrification and NO_3 seepage. Deep roots (native forest) for top 38% of slope. Shallow roots (pasture) for lower 62% of slope.	As for scenario 1, except deep roots (trees) added to bottom 25 m of slope (SMZ).	Hypothetical low slope, high rainfall and NO_3, and higher temperature (18 ^{o}C). Vegetation as for scenario 1, i.e. no trees in SMZ.	As for scenario 3, except deep roots (trees) added to bottom 25 m of slope (SMZ).	As for scenario 4, plus enhanced carbon supply, less anoxic conditions, and double the width trees in the SMZ (50 m).
Slope length (m)	515.2				
Duration (d)	365				
Water fluxes	Daily rainfall and potential transpiration assuming no evaporation				
Root water uptake	Feddes model parameters (no solute stress): P0 -10, POpt -25, P2H -300, P2L -1000, P3 -1100, r2H 0.5, r2L 0.1				
Spatial nodes	Horizontal: 96 (2.5 m apart at the bottom of slope to 5.7 m apart at the top of slope) Vertical: 21 (0.027 m apart at the top of the soil profile to 0.27 m apart at the bottom of the soil profile)				
Time steps (d)	0.01–1				
HYDRUS units	cm length, mg l^{-1} liquid concentration, mg kg^{-1} solid concentration, g cm^{-3} soil bulk density				
Slope (^{O})	17.4		2.0		
Rainfall (mm)	572		1200		
Soil horizons: thickness (m), texture[a], K_{sat} (cm d^{-1})	Horizon 1: 0.95, sandy loam, 106.1 Horizon 2: 1.41, silty clay loam, 1.68 Horizon 3: 0.64, silty clay, 0.48		Horizon 1: 0.95, sandy loam, 106.1 Horizon 2: 1.41, loamy sand, 350.2 Horizon 3: 0.64, sand, 1000		
Root depths native forest: pasture: SMZ (m)	3.0:0.5:0.5	3.0:0.5:3.0	3.0:0.5:0.5	3.0:0.5:3.0	3.0:0.5:3.0

[a] Texture as selected in HYDRUS from default options.

Table IV. Description of annual scenarios: salient CW2D inputs

Attribute	Values for all scenarios
Soil specific parameters (all horizons)	Bulk density 1.5 g cm^{-3}, Disp L 0.5, Disp T, 0.1, Fract 1, ThImob 0
Solute specific parameters (for solutes 1–13[a])	Difus W: 0.072, 0.0456, 0.0456, 0.0456, 0, 0, 0, 0.0801, 0.0801, 0.0801, 0.000801, 0.0000801, 0.05 Difus G: 769, 0, 0, 0, 0, 0, 0, 0, 0, 0, 0, 0, 0
Oxygen atmospheric boundary condition (mg l^{-1})	11
K_d for solutes 1–13	10^5, 10^6, 10^6, 10^6, 0, 0, 0, 10^6, 0, 0, 0, 10^7, 0
Maximum concentrations for uptake (mg l^{-1}	NH_4-N 560, NO_3-N 450, PO_4-P 1.4
Temperature	Set constant at 12.5 °C, no temperature dependence of reactions
Initial NO_3-N concentration	1 mg l^{-1} throughout the hillslope

[a] Solutes 1–13 in CW2D are 1 dissolved oxygen, 2 readily biodegradable organic matter, 3 slowly biodegradable organic matter, 4 inert organic matter, 5 heterotrophic organisms, 6 autotrophic *Nitrosomonas*, 7 autotrophic *Nitrobacter*, 8 NH_4, 9 NO_2, 10 NO3, 11 N_2, 12, PO_4, 13 tracer.

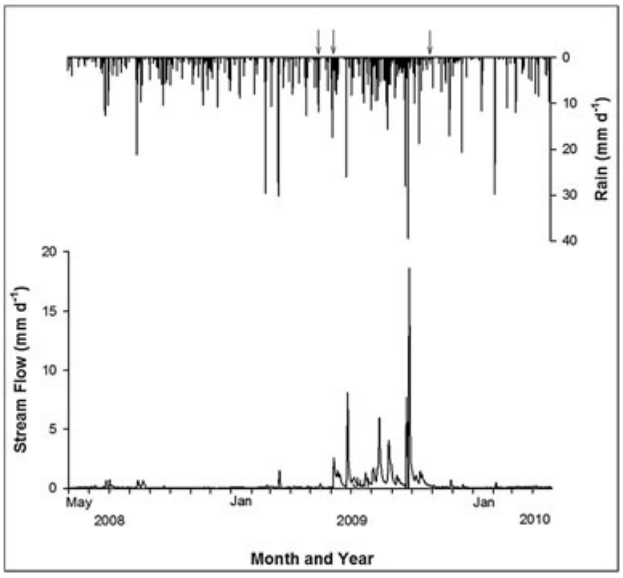

Figure 2. Rainfall and stream flow in the study catchment May 2008 to April 2010. Arrows indicate storms that were automatically sampled

Rain water and soil solution NO_3

Concentrations of NO_3-N in rain water were 0.029 mg l^{-1} in September 2009 and 0.059 mg l^{-1} in October 2009. Concentrations in soil solution were generally higher and ranged from the detection limit of 0.002 to 107 mg l^{-1} (Table V). These concentrations were consistent with similar measurements by others in Tasmania (Adams and Attiwill, 1991; Smethurst *et al.*, 2001). The highest concentrations of NO_3-N in soil solution were measured in the mid-slope pasture area in March 2010. Very low concentrations were more common in the up-slope forest area and the low-slope pasture-plantation SMZ area.

Leachate and water table NO_3 and oxygen

Leachate samples could only be obtained when water was freely draining below the root zone and while equipment was functioning. Water tables could be more reliably sampled, but in upper mid-slope pasture positions, a substantial water table was present only during the wettest period of 2009. Maximum concentrations of NO_3-N in leachate below the pasture root zone (0.5 m) were lower than those measured in soil solution in the root zone or the water table (Figure 3). Upper mid-slope pasture positions had the highest concentrations in leachate and the water table when sampled during May–Sept 2009. Concentrations of NO_3-N in the water table generally ranked upper mid-slope pasture > lower mid-slope pasture > low-slope buffer, suggesting that NO_3 was either removed as water drained down the slope, or that low-NO_3 water was added preferentially down-slope.

Concentrations of NO_3-N in stream water collected at 3- to 6-weekly intervals during each flow season were in the range <0.002–1.00 mg l^{-1}, with a peak in the middle (2008) or early (2009) part of that period, and thereafter concentrations decreased (data not presented). From storm 1 to storm 2, there was an increase in initial NO_3 concentration and a small decrease in peak NO_3 concentration, and storm 3 had substantially lower concentrations throughout the event than was observed in the two earlier storms. During storms 1 and 2, an increase in NO_3 concentration was measured that was preceded by a dilution early in the event. Also, during storm 3, an increase in concentration was observed, but preceding dilution was not observed as early concentrations were close to the detection limit anyway (0.002 mg l^{-1} NO_3-N; storm 3) (Figure 4). Peak concentrations followed peak flow by 1, 4, and 0 d after these three storms, respectively. Plots of concentration as a function of discharge showed that NO_3 concentrations increased with flow, with a clear anti-clockwise hysteresis pattern for storm 1, a predominantly anti-clockwise pattern for storm 2, and a mixed clockwise and anti-clockwise pattern for storm 3 (Figure 5).

The concentration of dissolved O_2 decreased from approximately 5 mg l^{-1} at the top of the water table, above which no denitrification would be expected, to levels near 2 mg l^{-1} at the bottom of the water table (Figure 6)

Mineralization, nitrification, and uptake

The rate of net N mineralization (NH_4 production) in laboratory incubations (Figure 7) weighted by area (forest 38.0%, mid-slope pasture 56.4%, low-slope pasture 5.6%) was 1.68 μg g^{-1} d^{-1}, of which 61.1% was nitrified

Table V. Summary of NO_3 concentrations in soil solution (0–10 cm depth) on three occasions

Slope position and concentration attribute	Nitrate concentration ($mg\,l^{-1}$)		
	10th September 2009	23rd November 2009	24th March 2010
Up-slope forest			
Median	0.12	<DL[a]	<DL
Minimum	0.03	<DL	< DL
Maximum	0.17	1.35	<DL
N	3	3	3
Mid-slope pasture			
Median	0.63	1.39	21.14
Minimum	<DL	0.50	<DL
Maximum	5.59	80.84	107.49
N	9	9	9
Low-slope pasture plantation (SMZ)			
Median	0.092	0.974	10.88
Minimum	0.044	0.342	1.71
Maximum	0.112	7.488	24.30
N	3	3	3

[a] <DL = less than detection limit of $0.002\,mg\,l^{-1}$

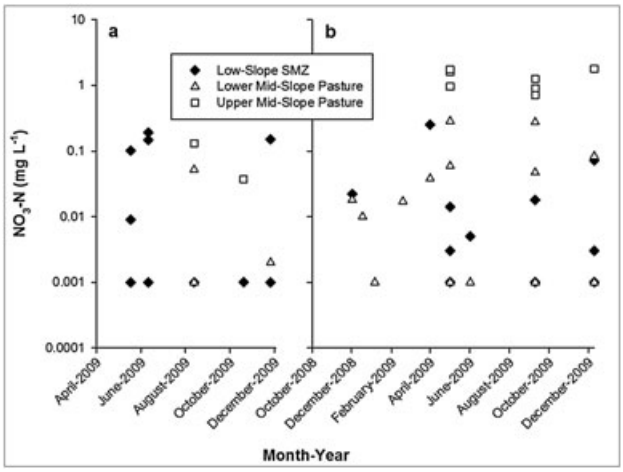

Figure 3. Nitrate concentrations in leachate (a) and the water table (b) in relation to slope position

(NO_3 production). High rates of net N mineralization in the forest area (Figure 7) were probably related to higher organic matter concentrations measured. The SNAP model estimated an annual rate of net N mineralization of $126\,kg\,ha^{-1}\,year^{-1}$ in the top 10 cm of soil (Table VI), with a minimum in July–August and maximum in January–February (data not shown). Applying the laboratory proportion of nitrification, and assuming half of all N mineralized and nitrified occurs in the top 10 cm of soil, NO_3 production was estimated to be $154\,kg\,N\,ha^{-1}\,year^{-1}$ (Table VI).

The measured rate of net N accumulation (assumed uptake) in above-ground pasture biomass was $231\,kg\,N\,ha^{-1}\,year^{-1}$ mid-slope and 328 low slope (Table VI), with an average N concentration of $17\,mg\,g^{-1}$. Assuming only $75\,kg\,N\,ha^{-1}\,year^{-1}$ was taken up by the forest, $177\,kg\,N\,ha^{-1}\,year^{-1}$ was taken up above-ground on average across the catchment, which equates to $155\,kg\,N\,ha^{-1}\,year^{-1}$ uptake of NO_3-N above- and below-ground for the whole of catchment.

Preferential flow

Simultaneous measurements of soil water content at 60–75 cm depth and rainfall provided many examples of rapid soil wetting at this depth in response to rainfall. In the example provided (Figure 8), one of four locations in a $30\,m^2$ area at this depth twice responded rapidly to rainfall, increasing soil water content on the second occasion from 0.26 to $0.30\,cm^3\,cm^{-3}$ over a period of 1.3 h, which suggests an effective vertical wetting front speed of at least $11\,m\,d^{-1}$ in some areas (probably through macropores), or a higher rate if it had a lateral flow component. Measured preferential flow is consistent with observed cracking of these surface soils during dry conditions.

Simulation of storm

Observed rainfall during 13–19 May had two storm peaks with a minor peak at 1 d into the event and the other at 3 d, with almost no rain for a half-day period in between (Figure 4). Flow analysis indicated, as expected, that baseflow was almost 100% of total flow at the start and end of the storm, and also about 2 d into the storm during the low-rain period (Figure 9 top). Baseflow gradually increased during the storm to a peak at 3.4 d, after which no rain fell. Baseflow simulated as seepage using the HYDRUS software was similar in trend and absolute value to that observed or predicted using flow analysis ($R^2 = 0.86$), except the initial rise in baseflow was simulated much earlier than that observed (Figure 9 bottom).

Measured concentrations of NO_3-N decreased from 0.10 to $0.01\,mg\,l^{-1}$ for the first day of storm 1, then increased and peaked at about $2.5\,mg\,l^{-1}$ on day 3

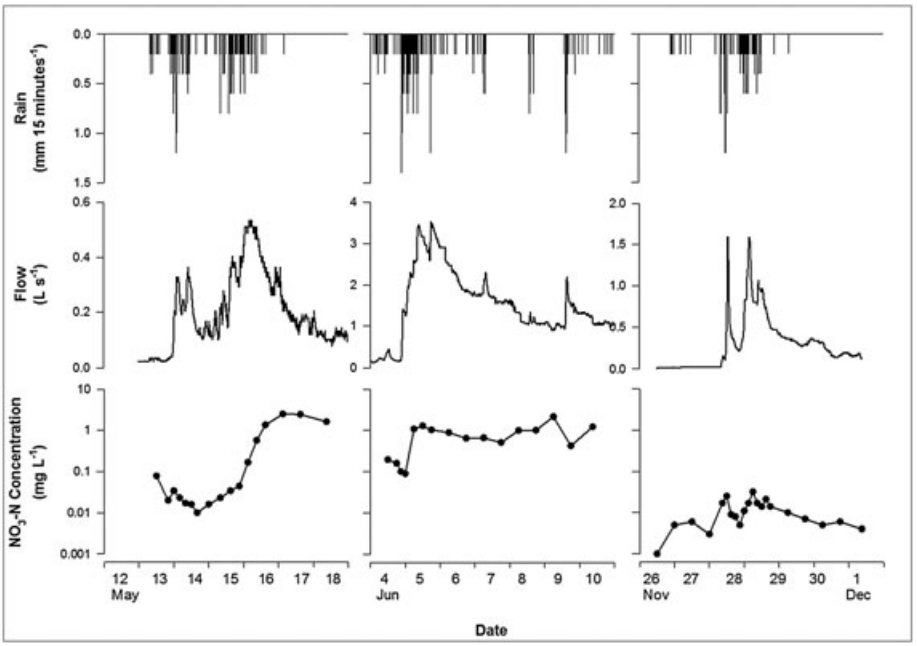

Figure 4. Patterns of rainfall, stream flow, and NO3 concentration during the three automatically sampled storms

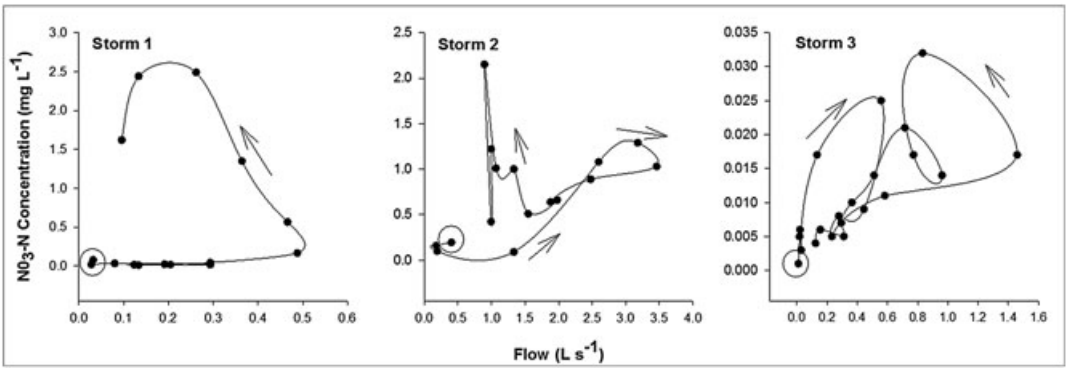

Figure 5. Concentration-flow (hysteresis) patterns of NO3 for the three storms (circles indicate starting points, arrows indicate directions of main loops)

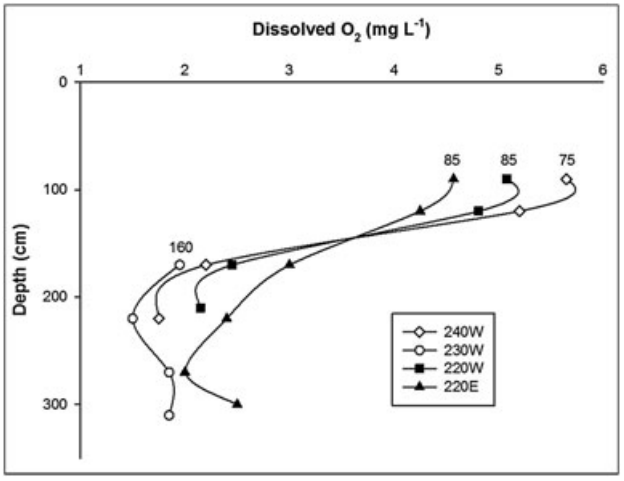

Figure 6. Profiles of dissolved O2 in the water table on 16th April 2009. Numbers indicate the depth of the surface of the water table at the time of sampling. Codes in the legend refer to location of piezometers: elevation (m) and the side of the catchment (E east, W west)

(Figure 10 top). If overland flow (i.e. quick flow) was assumed to contain no NO_3, the dilution effects during the second part of the storm were unrealistic, and observations were that concentrations in stream water continued to increase. A theoretical pattern of concentration in quick flow was found that, when combined with baseflow (i.e. slow flow), resulted in a similar simulated concentration pattern to that measured in stream flow (Figure 10 bottom). These results suggest that simulated concentrations in overland flow dominated the concentration pattern when significant overland flow was predicted, and at other times the concentration pattern was dominated by seepage concentrations.

Annual simulations and SMZ plantation effect

The runoff coefficient (discharge as a percent of rainfall) during the dry year was simulated to be 3%, compared to 4% measured. Whereas in the wet year both

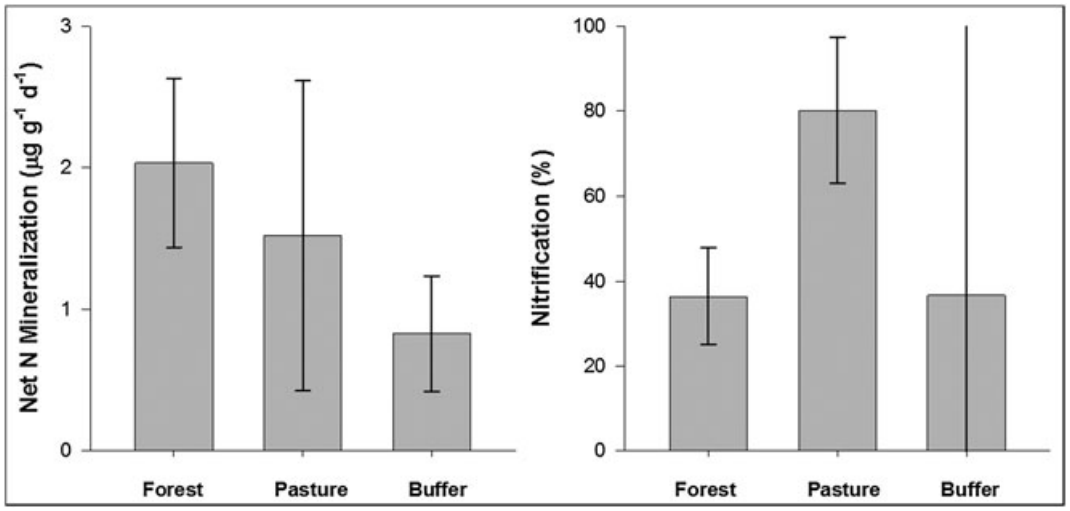

Figure 7. Net N mineralization and percentage nitrification measured on samples from three parts of the catchment (0–10 cm depth; $n = 3$ for forest and buffer samples, $n = 9$ for pasture samples). Bars are 95% confidence intervals of the mean

Table VI. Summary of annual rates of mineralization, nitrification, and uptake measured or estimated in the study catchment

Process	Value
Mineralization–Nitrification	
Laboratory (measured):-	
Net N mineralization ($\mu g\,g^{-1}\,d^{-1}$)	1.68
Nitrification (%)	61.1
Field (SNAP model estimate):-	
Net N mineralization ($kg\,N\,ha^{-1}\,year^{-1}$, 0–10 cm depth)	126.3
Nitrification ($kg\,N\,ha^{-1}\,year^{-1}$, 0–10 cm depth)	77.2
Nitrification ($kg\,N\,ha^{-1}\,year^{-1}$, total soil profile)	154
Uptake	
Forest above-ground N accumulation ($kg\,N\,ha^{-1}\,year^{-1}$, assumed)	75
Pasture above-ground N accumulation ($kg\,N\,ha^{-1}\,year^{-1}$, measured)	231
Buffer pasture above-ground N accumulation ($kg\,N\,ha^{-1}\,year^{-1}$, measured)	328
Catchment above-ground total N uptake ($kg\,N\,ha^{-1}\,year^{-1}$)	177
Catchment above- and below-ground NO_3-N uptake ($kg\,N\,ha^{-1}\,year^{-1}$)	155

Major assumptions and sources of error are (1) that it is valid to apply the SNAP model with its input errors and inherent errors of estimates, (2) the proportion of nitrification measured in the laboratory applies to the field, (3) the proportion of total-profile net N mineralization is double that in the top 10 cm of the soil profile, (4) net N accumulated in plant biomass approximates uptake, (5) above-ground N uptake is 70% of total-plant N uptake, (6) NH_4 and NO_3 are taken up in the same proportions as present in soil.

observed and simulated runoff coefficients were 24%. Hence, the simulated hydrological cycle was similar to that observed in both years.

Model simulations were used to estimate rates of denitrification and seepage, and the change in the soil NO_3 pool (Table VII). By varying some parameters and initial conditions in the model, water fluxes, nitrification, and uptake were tuned to approximate observed values. Predicted denitrification was only 2% of the nitrification flux for both years (Table VII), and it was predicted to occur across the hillslope where a water table existed (data not presented). Predicted and observed seepage of NO_3 to the stream was $< 0.05\,kg\,N\,ha^{-1}\,year^{-1}$ for the dry year. In the wet year, predicted seepage of NO_3 was $1.6\,kg\,N\,ha^{-1}\,year^{-1}$ compared to an observed value of $0.3\,kg\,N\,ha^{-1}\,year^{-1}$. Simulated flow velocity (magnitude and direction) depended on time and position (data not presented), but, during low and moderate rainfall events, flow directions were generally vertical down in the unsaturated zone and laterally down-slope in the saturated zone. High rainfall events were associated with an increase in lateral, down-slope flow in surface soil.

Scenario 2 suggested that establishment of an SMZ plantation would have little effect on denitrification, but it would increase N uptake and thereby reduce N concentrations in stream water (Table 7I, Figure 11). Scenario 3 was tuned to be more conducive to denitrification, but, while denitrification increased, it remained a minor source of N loss from this system. Scenario 4, which also was tuned to be more conducive to denitrification, and unlike Scenario 3 included an SMZ plantation, yielded similar results. In Scenario 5, when the simulation was tuned to be more oxygenated, rates of denitrification decreased substantially (72% decrease) compared to Scenarios 3 and 4, suggesting what might occur if an SMZ plantation increased transpiration, reduced water table depths, and increased aeration.

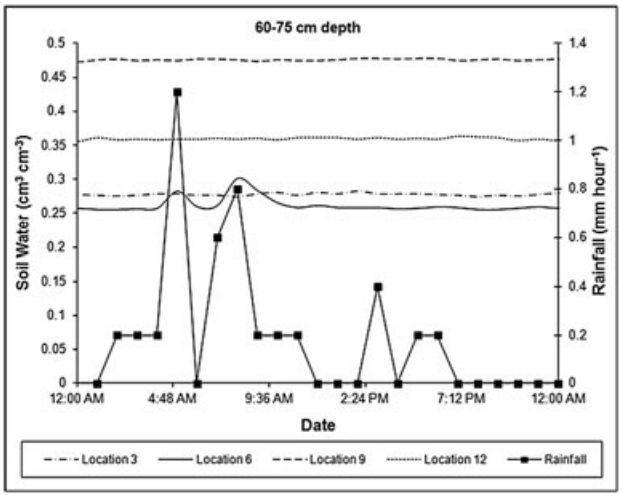

Figure 8. Volumetric soil water content (60–75 cm depth) at four locations in relation to rainfall on the 2nd September 2008. Note that water content at one location responded almost instantaneously to peaks in rainfall, indicating preferential flow from rainfall falling at the surface, but no response was seen at other locations

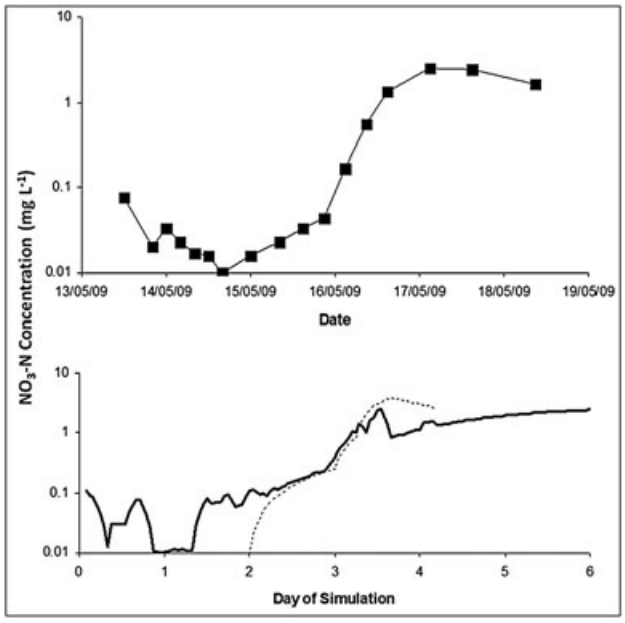

Figure 10. Measured (top) and simulated (bottom, solid line) concentrations of NO3-N in stream water at the Willow Bend site. Assumed concentrations of NO3-N in overland flow (quick flow) are indicated by the broken line in the bottom graph

DISCUSSION

NO_3 concentrations in most soils vary seasonally due to the interactive effects of microbial activity (as affected by rainfall and temperature), plant uptake, leaching, and denitrification. Pasture and forest soils in Tasmania are no exception (Moroni *et al.*, 2002). Management practices are also important, particularly those that affect organic matter quality and quantity, e.g. stocking rates of cattle and sheep, and inputs from mineral fertilizers and manures (Holz, 2010). Delivery of NO_3 to streams is largely a function of topography, soil type, land management, and the amount and pattern of rainfall. Base-flow concentrations of NO_3 in streams with excessive N inputs

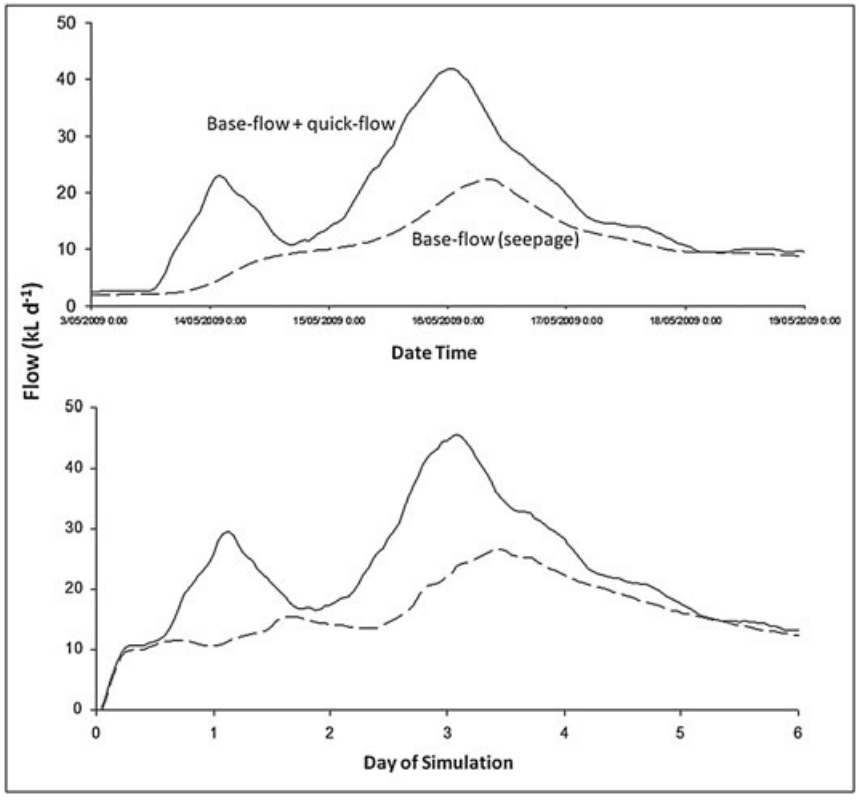

Figure 9. Observed flow (top) in the Willow Bend catchment 13–19 May 2009 and its simulation (bottom) using quick-flow analysis and the HYDRUS software

Table VII. Simulated water and NO_3 dynamics at the Willow Bend site for the one-year periods starting May 2008 and May 2009. Model inputs were as described in Tables III and IV, scenario 1. Various parameters were tuned to achieve the required water balance and rates of nitrification and NO_3 uptake for the dry year. These tuned values are shaded grey. For the dry year, rates of denitrification and seepage, and the soil NO_3 pool are model predictions. For the wet year, only precipitation was changed

Pool or Flux	May 2008 to April 2009	May 2009 to April 2010
Water Balance (mm)		
Precipitation	572	814
Evapotranspiration	616	644
Overland flow	15	151
Seepage to stream	3	19
Runoff coefficient (%)	3	24
Soil water change	−63	−77
Nitrogen balance (kg N ha^{-1} year^{-1})		
Nitrification	154.1	130.7
Uptake	127.3	98.1
Denitrification	2.5	2.5
Stream-flow NO_3	0.0	1.6
Stream NO_3-N concentration (mg l^{-1}; flow weighted)	0.02	0.81

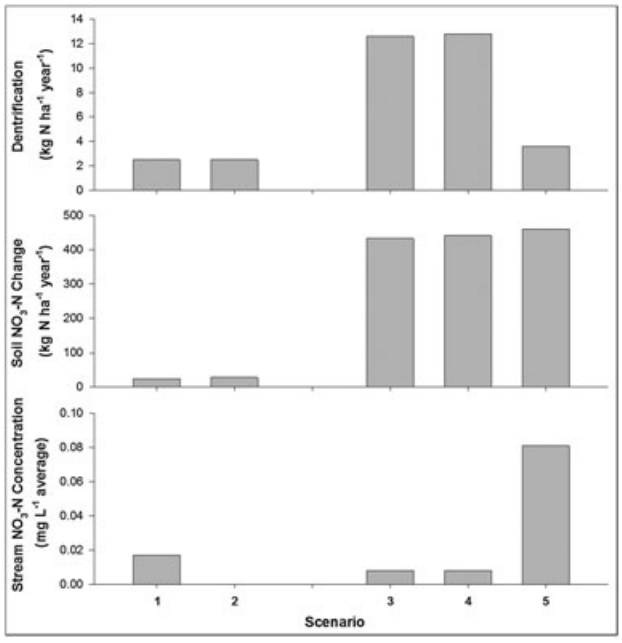

Figure 11. Simulated denitrification flux, change in the soil NO_3-N pool, and average concentration of NO3-N in stream water for scenarios 1–5. Scenarios 1 and 2 are for the study site without and with an SMZ plantation, respectively. Scenarios 3–5 are for hypothetical scenarios more conducive to denitrification, i.e. higher rainfall, lower slope, and more soil organic matter (see Table II for detail description)

can be as high as 30 mg l^{-1} (Hefting *et al*., 2006; Schilling *et al*., 2006; Huang *et al*., 2009; Kato *et al*., 2009), but less-intensively managed agricultural systems and forested catchments commonly have much lower concentrations (e.g. Verburg *et al*., 2012; Vink *et al*., 2007). Where flushing patterns are observed, NO_3 concentrations during events can increase several fold and up to 20 mg l^{-1} above base-flow concentrations (Ohrui *et al*., 1998; Ocampo *et al*., 2006; Poor and McDonnell, 2007; Rusjan *et al*., 2008). In an Australian study, NO_3 flushing was also observed, with peak concentrations early in the flow season reaching 5 mg l^{-1} with low intensity grazing and 24 mg l^{-1}with a forest plantation (Vink *et al*., 2007). In that study, and in Holz (2010), peak- and base-flow concentrations progressively decreased during most flow seasons. Our observed patterns of NO_3 concentration, were generally low and peaked early in the flow season. These patterns were

Table VIII. Simulated water and NO_3 dynamics at the study site (scenario 1) and with trees hypothetically in the SMZ (scenario 2). Also shown are other hypothetical scenarios with (compared to the study site) lower slope, wetter soil, and higher NO_3 concentrations, i.e. more conducive to denitrification. The model required various parameters to be tuned to achieve the required water balance and rates of nitrification and NO_3 uptake in the pasture base cases (scenarios 1 and 3). To simulate tree vegetation in the SMZ (scenarios 2 and 4,) roots were extended to the full depth of the soil profile in the SMZ (lowest 25 m of slope). A further scenario (scenario 5) included extending the width of the SMZ to 50 m and reduced the level of anoxia in the water table from 1 to 5 mg l^{-1} O_2. Tuned values are shaded grey. Denitrification, soil NO_3 change, and stream water NO_3 are shown in Figure 11.

Pool or Flux	Study site scenarios		Higher nitrate scenarios		
	Pasture SMZ (scenario 1)	25 m SMZ trees (scenario 2)	Pasture SMZ (scenario 3)	25 m SMZ trees (scenario 4)	50 m SMZ trees and less anoxic (scenario 5)
Water balance (mm)					
Precipitation	572	572	1200	1200	1200
Evaporation	0	0	0	0	0
Transpiration	616	625	811	806	843
Overland flow	15	15	170	189	162
Seepage	3	0	228	200	173
Soil water	−63	−69	8	41	31
Runoff coeff. (%)	3	3	32	31	28
Nitrogen balance (kg ha^{-1} year^{-1})					
Nitrification	154.1	152.6	701.7	702.6	729.7
Uptake	127.3	121.5	255.9	247.4	265.9
Seepage	0.0	0.0	0.0	0.0	0.3

consistent with mixed land-use catchments where low-intensity management includes low rates of N fertilization. More intense land use would probably have led to higher NO_3 concentrations throughout the flow season (Holz, 2010; Ignatius *et al.*, 2012)

In flushing systems, initial dilution of NO_3 concentrations during an event has been observed in water of headwater streams (Poor and McDonnell, 2007; Kato *et al.*, 2009), which can be attributed to direct stream or near-stream interception of low-NO_3 rain water. Regardless if this dilution effect occurs, increasing concentration during and shortly after the event indicates NO_3-enriched water reaching the stream in interflow (Rusjan *et al.*, 2008; Inamdar *et al.*, 2009) or overland flow (McColl and Gibson, 1979; Cooke and Cooper, 1988; Robertson and Nash, 2008) draining high-NO_3 surface soils (Robertson and Nash, 2008). On a seasonal or annual time scale, repeated flushing tends to deplete the soil profile of NO_3 and concentrations in stream water trend downwards (Poor and McDonnell, 2007). These patterns were also evident in our data, as we observed (1) a hysteresis response during storms whereby low NO_3 at the onset of storm flow shifted to high NO_3 at maximum flow or during flow recession (Figures 4–5) and (2) generally decreasing concentrations during the season. These patterns are typical of NO_3 flushing systems.

The flushing effect appears to have been facilitated by preferential flow within surface soil, because elevated flows and NO_3 concentrations persisted beyond the occurrence of rainfall (Figure 4) and very high wetting front velocities in some locations resulted in rapid delivery of rainfall to the base of the soil profile (Figure 8). The potential for preferential flow in surface soil to facilitate the quick delivery of PO_4 to streams has been recognized for many years (Stamm *et al.*, 1998; Stevens *et al.*, 1999), and recently measured on texture-contrast soils in southern Tasmania (Hardie *et al.*, 2011). Our results demonstrate and quantify this process for NO_3. Although the CW2D configuration of HYDRUS precludes the use of preferential flow, graphical output shows that water velocities predicted across the hillslope were maximal after high rainfall and in the bottom part of the surface-soil horizon where the highest saturated hydraulic conductivity was specified in an attempt to mimic preferential flow. These flow patterns were also consistent with a surface-soil-NO_3-flushing hypothesis.

Several authors have classified within-event concentration-flow patterns (hysteresis), as a diagnostic tool for interpreting catchment processes (Evans and Davies, 1998; Holz, 2010). Results here demonstrate that the pattern of hysteresis varied considerably between storm events, as also reported by numerous other studies (Figure 5; Petrone *et al.*, 2007; Rusjan *et al.*, 2008). Concentration-flow hysteresis alone therefore cannot be used to infer mechanisms within a catchment, but such patterns remain a useful way to illustrate and compare the outcomes of catchment processes.

Dissolved oxygen concentrations decreased with depth in the water table to values low enough to be conducive to denitrification ($2\,mg\,l^{-1}$; Figure 6; Körner and Zumft, 1989). NO_3 concentrations in the saturated zone were also noted to be highest up-slope, which is consistent with denitrification being most advanced in deeper water down-slope. Hence, it is postulated that denitrification rates increased with water table depth and lower-slope positions.

Modelling of catchment processes that deliver NO_3 to a stream has increased in sophistication during recent years by the inclusion of spatial and temporal detail of water flows and soil NO_3 concentrations (Ignatius *et al.*, 2012; Weiler and McDonnell, 2006), or with detailed N turnover (Hong *et al.*, 2006; Huang *et al.*, 2009). In this manuscript, we demonstrate how the major processes controlling NO_3 concentrations in soil can be combined with detailed hillslope hydrologic modelling to simulate NO_3 delivery to a stream across short and long time scales. This development offers many opportunities for virtual experiments of land-use change such as encouraged by Weiler and McDonnell (2006) and simulation of catchment observations (Figure 9, Table VII).

Our virtual experiment included a forest plantation with a 50 m wide SMZ that increased transpiration (4%), which in-turn decreased stream flows (24%), and increased NO_3 uptake (4%). However, as nitrification increased (4%) and denitrification decreased (75%), NO_3 concentrations in stream water increased (800%), which in this scenario still remained low ($0.08\,mg\ NO_3\text{-}N\,l^{-1}$) (Table 7I, Figure 11). This scenario demonstrates the complexity of interactions that need to be considered when speculating about the mitigation effect of SMZ plantations. These scenarios were not fully validated, but a paired catchment experiment has been established to determine the water quality and stream flow effects of this practice (Smethurst *et al.*, 2009), and most of the water and NO_3 fluxes in these scenarios were similar to those measured in the catchment, i.e. rainfall, streamflow, nitrification, uptake, and seepage to the stream.

Results presented challenge the assertion of Rassam *et al.* (2008) that tree establishment in an SMZ (riparian zone) will promote denitrification and thereby reduce NO_3 delivery to the stream. This effect could only occur if trees did not alter the soil water and NO_3 status and if they increased soil C concentrations, which would in turn promote denitrification. Conversely, Fellows *et al.* (2007), in a paired-site study at various locations in Australia, found that trees in SMZs did not increase soil carbon concentrations or rates of denitrification.

It is possible that trees will increase transpiration (Vink *et al.*, 2007) and NO_3 uptake rates (Zhang *et al.*, 2010), which would lead to reduced rates of denitrification. Observations and modelling by Speiran (2010) also indicate that NO_3 uptake by vegetation in riparian zones and buffers should be given more emphasis than it has received so far. This author also pointed out that most increased carbon availability brought about by forests is in surface soils that are aerated and unlikely to promote denitrification, except during seasonal or temporary flooding. However, our results suggest that increased

nitrification, soil NO_3 concentrations, and leaching as a result of trees might negate the NO_3-mitigating effects of uptake. Our current working hypothesis therefore is that, if trees established in SMZs mitigate NO_3 delivery to streams, if at all, it will be via increased NO_3 uptake and not via enhanced denitrification, but increased nitrification is a risk to these mitigating processes. This hypothesis was generated by virtual experiments (Table 7I, Figure 11). The N retention capacity of the SMZ might need to be renewed periodically, however, by removing N in plant material through tree harvesting. 'Crash' grazing of remnant pasture (short duration and intense) during dry periods might also be an option when there is a low risk of stream contamination, but manure inputs could negate forage outputs. Managed burning could also be considered, but could present a risk of P and sediment contamination of stream water and damage to trees.

In this study, the observed patterns of NO_3 concentration and flow were consistent with a NO_3 flushing hypothesis, i.e. storms delivered high NO_3 in surface water within 1–2 days from the onset of the storm. Maximum NO_3 concentrations in stream water during early season storms were generally high considering the lack of use of fertilizers and other intensive inputs, and despite the relatively high-flow nature of the season in which the storms were automatically sampled. Overall, observed patterns of flow and concentration during a storm could be simulated using flow analysis and the HYDRUS software. In its first application to hillslope NO_3 dynamics, the HYDRUS-CW2D model was used to simulate catchment pools and fluxes of NO_3. This modelling predicted that denitrification occurred throughout the catchment where a water table occurred. However, denitrification accounted for only a small component of NO_3 production. This prediction was consistent with other flux measurements and observed concentrations of NO_3 in the water table that ranged from 2 mg l^{-1} up-slope to 0.001 mg l^{-1} down-slope. The hypothetical addition of an SMZ containing a forest plantation with deep tree roots increased water and NO_3 uptake but also resulted in increased nitrification and a minor decrease in denitrification. Major sources of error in this analysis include measurements of catchment-scale NO_3 pools and fluxes, and several assumptions that were necessary to simplify simulations. Nevertheless, the combined analysis was useful for improving our understanding of complex water and NO_3 dynamics in this headwater catchment, and for indicating directions and challenges for future measurements and modelling of hillslope NO_3. A 2D hillslope model as shown in this research might be satisfactory for many types of catchment applications and therefore warrants further testing.

ACKNOWLEDGEMENTS

We thank variously for support, assistance, and advice: Chris White, Rob Smith, Private Forests Tasmania, Daniel Neary, Landscape Logic CERF Hub, CRC for Forestry, CSIRO Sustainable Agriculture Flagship, CSIRO Water for a Healthy Country Flagship, and the Victorian Department of Primary Industries. We also thank Marcus Hardie, Sébastien Lamontagne, David Drew, and two anonymous reviewers for comments on earlier versions of this manuscript.

REFERENCES

Adams MA, Attiwill PM. 1991. Nutrient balances in forests of northern Tasmania. 1. Atmospheric inputs and within-stand cycles. *Forest Ecology and Management* **44**: 93-113. DOI: 10.1016/0378-1127(91)90001-C.

Chiwa M, Ide J, Maruno R, Higashi N, Otsuki K. 2010. Effects of storm flow samplings on the evaluation of inorganic nitrogen and sulphate budgets in a small forested watershed. *Hydrological Processes* **24**: 631-640. DOI: 10.1002/hyp.7557.

Cooke JG, Cooper AB. 1988. Sources and sinks of nutrients in a New Zealand hill pasture catchment III. Nitrogen. *Hyrological Processes* **2**: 135-149. DOI: 10.1002/hyp.3360020204.

Creed IF, Band LE. 1998. Exploring functional similarity in the export of nitrate-N from forested catchments: a mechanistic modeling approach. *Water Resources Research* **34**: 3079-3093. DOI: 10.1029/98WR02102.

Dosskey MG, Vidon P, Gurwick NP, Allan CJ, Duval TP, Lowrance R. 2010. The role of riparian vegetation in protecting and improving chemical water quality in streams. *Journal of the American Water Resources Association* **46**: 261-277. DOI: 10.1111/j.1752-1688.2010.00419.x.

Evans C, Davies TD. 1998. Causes of concentration/discharge hysteresis and its potential as a tool for analysis of episode hydrochemistry. *Water Resources Research* **34**: 129-137. DOI: 10.1029/97WR01881.

Fellows C, Hunter H, Grace M. 2007. Chapter 4, Managing diffuse nitrogen loads: in-stream and riparian zone nitrate removal. In *Salt, Nutrient, Sediment and Interactions: Findings from the National River Contaminants Program*, Lovett S, Price P, Edgar B (eds). :Land and Water Australia: Canberra, Australia; 43–58. ISBN 978-1-921253-68-3.

Hardie MA, Cotching WE, Doyle RB, Holz G, Lisson S, Mattern K. 2011. Effect of antecedent soil moisture on preferential flow in a texture-contrast soil. *Journal of Hydrology* **398**: 191-201. DOI: 10.1016/j.jhydrol.2010.12.008.

Hefting M, Beltman B, Karssenberg D, Rebel K, van Riessen M, Spijker M. 2006. Water quality dynamics and hydrology in nitrate loaded riparian zones in the Netherlands. *Environmental Pollution* **139**: 143-156. DOI: 10.1016/j.envpol.2005.04.023.

Holz GK. 2010. Sources and processes of contaminant loss from an intensively grazed catchment inferred from patterns in discharge and concentration of thirteen analytes using high intensity sampling. *Journal of Hydrology* **383**: 194–208. DOI: 10.1016/j.jhydrol.2009.12.036.

Hong B, Weinstein DA, Swaney DP. 2006. Assessment of ozone effects on nitrate export from Hubbard Brook Watershed 6. *Environmental Pollution* **141**: 8-21. DOI: 10.1016/j.envpol.2005.08.030.

Huang S, Hesse C, Krysanova V, Hattermann FF. 2009. From meso- to macro-scale dynamic water quality modelling for the assessment of land use change scenarios. *Ecological Modelling* **220**: 2543-2558. DOI: 10.1016/j.ecolmodel.2009.06.043.

Ignatius GAMN, Heinen M, Heesmans HIM, Thissen JTNM, Groenendijk P. 2012. Effectiveness of Unfertilized Buffer Strips for Reducing Nitrogen Loads from Agricultural Lowland to Surface Waters. *Journal of Environmental Quality* **41**: 322-333. DOI: 10.2134/jeq2010.0545

Inamdar S, Rupp J, Mitchell M. 2009. Groundwater flushing of solutes at wetland and hillslope positions during storm events in a small glaciated catchment in western New York, USA. *Hydrological Processes* **23**: 1912-1926. DOI: 10.1002/hyp.7322.

Katsuyama M, Ohte N, Kobashi S. 2001. A three-component end-member analysis of streamwater hydrochemistry in a small Japanese forested headwater catchment. *Hydrological Processes* **15**: 249-260. DOI: 10.1002/hyp.155.

Kato T, Kuroda H, Nakasone H. 2009. Runoff characteristics of nutrients from an agricultural watershed with intensive livestock production. *Journal of Hydrology* **368**: 79-87. DOI: 10.1016/j.jhydrol.2009.01.028.

Körner H, Zumft WG. 1989. Expression of denitrification enzymes in response to the dissolved oxygen level and respiratory substrate in continuous culture of *Pseudomonas stutzeri*. *Applied and Environmental Microbiology* **55**: 1670-1676.

Kralisch S, Krause P. 2006. JAMS – A framework for natural resource model development and application. In *Proceedings of the iEMSs Third Biannual Meeting Summit on Environmental Modelling and Software*, Voinov A, Jakeman A, Rizzoli AE (eds). International Environmental Modelling and Software Society: Burlington; USA. Available at: http://www.mssanz.org.au/modsim09/C3/fischer.pdf (accessed 9April 2012).

Krause P, Bäse F, Bende-Michl U, Fink W, Pfennig B. 2006. Multiscale investigations in a mesoscale catchment – hydrological modelling in the Gera catchment. *Advances in Geoscience* **9**: 53-61. DOI: 10.5194/adgeo-9-53-2006.

Langergraber G, Šimůnek J. 2005. Modeling Variably Saturated Water Flow and Multicomponent Reactive Transport in Constructed Wetlands. *Vadose Zone Journal* **4**: 924–938. DOI: 10.2136/vzj2004.0166.

Langergraber G, Šimůnek J. 2012. Reactive Transport Modeling of Subsurface Flow Constructed Wetlands Using the HYDRUS Wetland Module. *Vadoze Zone Journal*, in press. DOI: 10.2136/vzj2011.0104.

Lowther JR. 1980. Use of a single acid-peroxide digest for the analysis of *Pinus radiata* needles. *Communications in Soil Science and Plant Analysis* **11**: 175-188. DOI: 10.1080/00103628009367026.

Lyne VD, Hollick M. 1979. Stochastic time-variable rainfall runoff modelling. In *Proceedings, Hydrology and Water Resources Symposium*, Perth, 1979. National Committee on Hydrology and Water Resources of the Institution of Engineers: Australia; 89-92.

McColl RHS, Gibson AR. 1979. Downslope movement of nutrients in hill pasture, Taita, New Zealand. *New Zealand Journal of Agricultural Research* **22**: 151-161. DOI: 10.1080/00288233.1979.10420855.

Moroni MT, Smethurst PJ, Holz GK. 2002. Nitrogen fluxes in surface soils of young Eucalyptus nitens plantations in Tasmania. *Australian Journal of Soil Research* **40**: 543-553. DOI: 10.1071/SR01024.

Moroni MT, Smethurst PJ, Holz PJ. 2004. Indices of soil nitrogen availability in five Tasmanian *Eucalyptus nitens* plantations. *Australian Journal of Soil Research* **42**: 719-725. DOI: 10.1071/SR03145.

Neary DG, Smethurst PJ, Baillie BR, Petrone KC, Cotching WE, Baillie CC. 2010. Does tree harvesting in streamside management zones adversely affect stream turbidity? - Preliminary observations from an Australian case study. *Journal of Soils and Sediments* **10**: 652-670. DOI: 10.1007/s11368-010-0234-2.

Ocampo CJ, Sivpalan M, Oldham C. 2006. Hydrological connectivity of upland-riparian zones in agricultural catchments; implications for turnoff generation and nitrate transport. *Journal of Hydrology* **331**: 643-658. DOI: 10.1016/j.jhydrol.2006.06.010.

Ohrui K, Mitchell MJ. 1998. Stream water chemistry in Japanese forested watersheds and its variability on a small regional scale. *Water Resources Research* **34**: 1553-1561. DOI: 10.1029/98WR00918.

Ohte N, Tokuchi N, Shibata H, Tsujimura M, Tanaka T, Mitchell M. 2001. Hydrobiogeochemistry of forest ecosystems in Japan: major themes and research issues. *Hydrological Processes* **15**: 1771-1789. DOI: 10.1002/hyp.239.

Paul KI, Polglase PJ, O'Connell AM, Carlyle JC, Smethurst PJ, Khanna PK. 2002. Soil nitrogen availability predictor (SNAP): A simple model for predicting mineralisation of nitrogen in forest soils. *Australian Journal of Soil Research* **40**: 1011-1026. DOI: 10.1071/SR01114.

Petrone KC, Hinzman LD, Shibata H, Jones JB, Boone RD. 2007. The influence of fire and permafrost on sub-arctic stream chemistry during storms. *Hydrological Processes* **21**: 423-434. DOI: 10.1002/hyp.6247.

Poor AJ, McDonnell JJ. 2007. The effect of land use on stream nitrate dynamics. *Journal of Hydrology* **332**: 54-68. DOI: 10.1016/j.jhydrol.2006.06.022.

Rasiah V, Armour JD, Cogle AL, Florentine SK. 2010. Nitrate import-export dynamics in groundwater interacting with surface-water in a wet-tropical environment. *Australian Journal of Soil Research* **48**: 361-370. DOI: 10.1071/SR09120.

Rassam DW, Pagendam DE, Hunter HM. 2008. Conceptualisation and application of models for groundwater-surface water interactions and nitrate attenuation potential in riparian zones. *Environmental Modelling and Software* **23**: 859-875. DOI: 10.1016/j.envsoft.2007.11.003.

Rayment GE, Higginson FR. 1992. *Australian Laboratory Handbook of Soil and Water Chemical Methods*. Inkata Press: Melbourne, Australia.

Robertson FA, Nash DM. 2008. Phosphorus and nitrogen in soil, plant, and overland flow from sheep-grazed pastures fertilized with different rates of superphosphate. *Agricultural Ecosystems and Environment* **126**: 195-208. DOI: 10.1016/j.agee.2008.01.023.

Rozemeijer JC, Broers HP, van Geer FC, Bierkensa MFP. 2009. Weather-induced temporal variation in nitrate concentrations in shallow groundwater. *Journal of Hydrology* **378**: 119–127. DOI: 10.1016/j.jhydrol.2009.09.011.

Rusjan S, Brilly M, Mikos M. 2008. Flushing of nitrate from a forested watershed: an insight into hydrological nitrate mobilization mechanisms through seasonal high-frequency stream nitrate dynamics. *Journal of Hydrology* **354**: 187-202. DOI: 10.1016/j.jhydrol.2008.03.009.

Schilling KE, Zhongwei L, Zhang Y-K. 2006. Groundwater-surface water interaction in the riparian zone of an incised channel, Walnut Creek, Iowa. *Journal of Hydrology* **327**: 140–150. DOI: 10.1016/j.jhydrol.2005.11.014.

Shabaga JA, Hill AR. 2010. Groundwater-fed surface flow path hydrodynamics and nitrate removal in three riparian zones in southern Ontario, Canada. *Journal of Hydrology* **388**: 52-64. DOI: 10.1016/j.jhydrol.2010.04.028.

Šimůnek J, van Genuchten MTh, Šenja M. 2008. Development and application of the HYDRUS and STANDMOD software packages and realted codes. *Vadose Zone Journal* **7**: 587-600. DOI: doi:10.2136/vzj2008.0012.

Smethurst PJ, Herbert AM, Ballard LM. 1997. A paste method for estimating concentrations of ammonium, nitrate and phosphate in soil solution. *Australian Journal of Soil Research* **35**: 209-225. DOI: 10.1071/S95040.

Smethurst PJ, Herbert AM, Ballard LM. 2001. Fertilization effects on soil solution chemistry in three eucalypt plantations. *Soil Science Society of America Journal* **65**: 795-804. DOI: 10.2136/sssaj2001.653795x.

Smethurst PJ, Langergraber G, Petrone KC, Holz GK. 2009. Hillslope and stream connectivity: simulation of concentration-discharge patterns using the HYDRUS model. In *Modsim09 Proceedings*. Modelling and Simulation Society of Australia and New Zealand: Australia. Available at: http://mssanz.org.au/modsim09/I14/smethurst_I14.pdf (accessed 9 April 2012).

Speiran G. 2010. Effects of groundwater-flow paths on nitrate concentrations across two riparian forest corridors. *Journal of the American Water Resources Association* **46**: 246-260. DOI: 10.1111/j.1752-1688.2010.00427.x.

Stamm C, Flühler H, Gächter R, Leuenberger J, Wunderli H. 1998. Preferential transport of phosphorus in drained grassland soils. *Journal of Environmental Quality* **27**: 515-522. DOI: 10.2134/jeq1998.00472425002700030006x.

Stevens DP, Cox JW, Chittleborough DJ. 1999. Pathways of phosphorus, nitrogen, and carbon movement over and through texturally differentiated soils, South Australia. *Australian Journal of Soil Research* **37**, 679-693. DOI: 10.1071/SR98082.

Stutter MI, Chardon WJ, Kronvang B. 2012. Riparian Buffer Strips as a Multifunctional Management Tool in Agricultural Landscapes: Introduction. *Journal of Environmental Quality* **41**: 297-303. DOI: 10.2134/jeq2011.0439.

Tilman D, Cassman KG, Matson PA, Naylor R, Polasky S. 2002. Agricultural sustainability and intensive production practices. *Nature* **418**: 671-677. DOI: 10.1038/nature01014.

Verburg K, Cresswell H, Bende-Michl U, Gibson J, Hairsine P. 2012. Spatial diagnosis of catchment water quality: using multiple lines of evidence. In *Landscape Logic*, Lefroy T, Curtis A, Jakeman A, McKee J (eds) CSIRO: Collingwood, Australia; 83-102.

Vink S, Ford PW, Kelly C, Turley C. 2007. Contrasting nutrient exports from a forested and an agricultural catchment in south-eastern Australia. *Biogeochemistry* **84**: 247-264. DOI: 10.1007/s10533-007-9113-3.

Weaver DM, Reed AEG, Grant J. 2001. Relationships between stream order and management priority: a water quality case study. In *Proceedings of the Third Australian Stream Management Conference*, Rutherfurd I, Sheldon E, Brierley G, Kenyon C (eds). August 27–29, Cooperative Research Centre for Catchment Hydrology: Brisbane; 647-652.

Weiler M, McDonnell JJ. 2006. Testing nutrient flushing hypotheses at the hillslope scale: A virtual experiment approach. *Journal of Hydrology* **319**: 339-356. DOI: 10.1016/j.jhydrol.2005.06.040.

Zhang X, Liu X, Zhang M, Dahlgren RA, Eitzel M. 2010. A review of vegetated buffers and a meta-analysis of their mitigation efficacy in reducing nonpoint source pollution. *Journal of Environmental Quality* **39**: 76-84. DOI: 10.2134/jeq2008.0496.

Zhu Q, Schmidt JP, Buda AR, Bryant RB, Folmar G. 2011. Nitrogen losses from a mixed land use watershed as influenced by hydrology and seasons. *Journal of Hydrology* **405**: 307-315. DOI: 10.1016/j.jhydrol.2011.05.028.

